Effect of Restricted Conformational Flexibility on the Permeation of Model Hexapeptides Across Caco-2 Cell Monolayers

Franklin W. Okumu,[1] Giovanni M. Pauletti,[1] David G. Vander Velde,[1] Teruna J. Siahaan,[1] and Ronald T. Borchardt[1,2]

Received September 4, 1996; accepted December 4, 1996

Purpose. To determine how restricted conformational flexibility of hexapeptides influences their cellular permeation characteristics.

Methods. Linear (Ac-Trp-Ala-Gly-Gly-X-Ala-NH_2; X = Asp, Asn, Lys) and cyclic (cyclo[Trp-Ala-Gly-Gly-X-Ala]; X = Asp, Asn, Lys) hexapeptides were synthesized, and their transport characteristics were assessed using the Caco-2 cell culture model. The lipophilicities of the hexapeptides were determined using an immobilized artificial membrane. Diffusion coefficients used to calculate molecular radii were determined by NMR. Two-dimensional NMR spectroscopy, circular dichroism, and molecular dynamic simulations were used to elucidate the most favorable solution structure of the cyclic Asp-containing peptide.

Results. The cyclic hexapeptides used in this study were 2–3 times more able to permeate (e.g., P_{app} = 9.3 ± 0.3 × 10^{-8} cm/sec, X = Asp) the Caco-2 cell monolayer than were their linear analogs (e.g., P_{app} = 3.2 ± 0.3 × 10_{-8} cm/sec, X = Asp). In contrast to the linear hexapeptides, the flux of the cyclic hexapeptides was independent of charge. The cyclic hexapeptides were shown to be more lipophilic than the linear hexapeptides as determined by their retention times on an immobilized phospholipid column. Determination of molecular radii by two different techniques suggests little or no difference in size between the linear and cyclic hexapeptides. Spectroscopic data indicate that the Asp-containing linear hexapeptide exists in a dynamic equilibrium between random coil and β-turn structures while the cyclic Asp-containing hexapeptide exists in a well-defined compact amphophilic structure containing two β-turns.

Conclusions. Cyclization of the linear hexapeptides increased their lipophilicities. The increased permeation characteristics of the cyclic hexapeptides as compared to their linear analogs appears to be due to an increase in their flux via the transcellular route because of these increased lipophilicities. Structural analyses of the cyclic Asp-containing hexapeptide suggest that its well-defined solution structure and, specifically the existence of two β-turns, explain its greater lipophilicity.

KEY WORDS: peptide delivery; conformation; Caco-2 cells; membrane permeability; NMR; CD.

[1] Department of Pharmaceutical Chemistry, 2095 Constant Ave., The University of Kansas, Lawrence, Kansas 66047.

[2] To whom correspondence should be addressed. (e-mail: borchardt@smissman.hbc.ukans.edu)

ABBREVIATIONS: AP, apical; BL, basolateral; PC, palmitoyl-DL-carnitine; Dod-resin, 4-(2′,4′-demethoxyphenyl-Fmoc-aminomethyl)-phenoxymethyl-polystyrene resin; Wang-resin, *p*-alkoxybenzyl alcohol resin; TFA, trifluoroacetic acid; NMR, nuclear magnetic resonance; CD, circular dichroism; HOHAHA, Homonuclear Hartmann-Hahn spectroscopy; ROESY, rotating frame nuclear Overhauser effect spectroscopy; ROE, rotating frame nuclear Overhauser effect cross peak.

INTRODUCTION

Recent advances in recombinant DNA technology and modern synthetic methodologies permit the production of large quantities of various peptides and peptide-mimetics possessing a diverse array of pharmacological effects (1). The clinical development of oral dosage forms of these peptidic drugs, however, has been restricted due to their poor permeation across the intestinal mucosa and their rapid enzymatic degradation (2–5).

Peptides and peptide-mimetics cross the intestinal mucosa by either the paracellular or the transcellular route (2). Most molecules that readily permeate the intestinal mucosa do so by passive diffusion via the transcellular route (6). The rate-limiting step for passive diffusion of peptides via the transcellular pathway is desolvation of the solute, which allows the molecule to enter the hydrophobic interior of the membrane (7). Burton and co-workers (8,9) have recently shown that reduction in the hydrogen-bonding potential of peptides and peptide-mimetics can improve their transcellular transport.

Some peptides and peptide-mimetics are reported to permeate the intestinal mucosa via the paracellular route (10–12). Since the paracellular pathway is an aqueous extracellular route across the epithelium, structural features that influence the flux of peptides via this pathway include molecular size, charge, and hydrophilicity (13). Of these structural features, molecular size probably plays the most significant role in determining the rate of paracellular flux due to the size restriction of the junctional complexes between intestinal epithelial cells (13–15). Recently, our laboratory (13) has clearly shown the importance of size in determining the paracellular flux of a series of peptides. The literature suggests that cyclic peptides that might have reduced molecular radii compared to linear peptides are more able to permeate the intestinal mucosa (e.g., cyclosporin) (16). However, it is unclear whether these favorable permeation characteristics are due to a reduction in the size of the peptide resulting in enhanced paracellular flux, or a change in other physicochemical properties (e.g., lipophilicity), which facilitates transcellular flux. To our knowledge, no literature examples exist in which direct comparisons have been made between the permeability characteristics of linear peptides and their cyclic analogs.

Therefore, the goal of this study was to determine how restricting conformational flexibility of model hexapeptides by cyclization affects their cellular permeation. For these studies, we prepared linear hexapeptides (Ac-Trp-Ala-Gly-Gly-X-Ala-NH_2; X = Asp, Asn, Lys) and cyclic analogs linked by the N- and C-terminal ends (cyclo[Trp-Ala-Gly-Gly-X-Ala]; X = Asp, Asn, Lys) and determined their ability to permeate Caco-2 cell monolayers, a model of the intestinal mucosa (17). Attempts were then made to correlate physicochemical properties (e.g., molecular size, lipophilicity) and/or solution structural features with their Caco-2 cell monolayer permeation characteristics.

MATERIALS AND METHODS

Materials

All Fmoc-amino acids and resins used were purchased form Bachem Biosciences Inc. (King of Prussia, PA). Palmitoyl-

0724-8741/97/0200-0169$12.50/0

DL-carnitine chloride (PC) and Hanks' balanced salts (modified) were purchased from Sigma Chemicals Co. (St. Louis, MO). Materials used to culture Caco-2 cells are described in detail elsewhere (18). All other reagents were purchased form TCI America (Harborgate, OR), Fisher Chemical Co. (Pittsburgh, PA), or Aldrich Chemical Co. (Milwaukee, WI).

Peptide Synthesis

All C- and N-terminally modified linear peptides were synthesized using Fmoc-protected amino acids attached to Dod-resin (19). Peptide chain elongation was accomplished by 1,3-diisopropylcarbodiimide/1-hydroxybenzotriazole coupling steps followed by deprotection with 20% piperidine in dimethylformamide. After the N-terminal Fmoc protection was removed, acetylation of the peptides was accomplished by incubation with acetic anhydride. Protecting groups were removed, and the peptides were cleaved from the resin by incubation in 90% trifluoroacetic acid (TFA), 5% ethanedithiol, and 5% *p*-cresol for 2 hours at room temperature. The peptides were precipitated from the crude reaction mixture with cold diethyl ether. The crude peptide was then dissolved in diluted acetic acid and lyophilized. The orthogonally protected peptides, H-Trp-Ala-Gly-Gly-Asp(OBzl)-Ala-OH (OBzl = benzyl ester), H-Trp-Ala-Gly-Gly-Lys(Z)-Ala-OH (Z = benzyloxycarbonyl) and H-Trp-Ala-Gly-Gly-Asn-Ala-OH were synthesized using Fmoc-protected amino acids attached to Wang resin (20). After the N-terminal Fmoc protection was removed, the peptide was cleaved from the resin by incubation in 90% TFA, 5% ethanedithiol, and 5% water. The cyclic peptides, cyclo[Trp-Ala-Gly-Gly-Asp(OBzl)-Ala], cyclo[Trp-Ala-Gly-Gly-Lys(Z)-Ala], and cyclo[Trp-Ala-Gly-Gly-Asn-Ala] were synthesized via head-to-tail cyclization of the linear peptides using a 10-fold molar excess of N,N-bis(2-oxo-3-oxazolidinyl) phosphinic chloride as the activating agent (21). The side chain protecting groups were removed from the Asp- and Lys-containing hexapeptides using hydrogen gas and 10% Pd/C as a catalyst.

Purification and Characterization

Crude peptides were purified using preparative HPLC (Rainin Instruments, Woburn, MA) equipped with a Dynamax column (21.2 × 250 mm) packed with spherical C_{18} silica gel (300 Å pore size, 12 μm particle size, Rainin Instruments, Woburn, MA), a Kratos 757 UV/Vis detector (Applied Biosystems, Inc., Foster City, CA) and a fraction collector (BioRad, Hercules, CA). Gradient elution of the peptides was performed at a flow rate of 5 mL/min from 5–40% (v/v) acetonitrile in water using TFA (0.1%, v/v) as an ion-pairing agent. Pure fractions were pooled and concentrated. All peptides were characterized by analytical HPLC, FAB-MS, and amino acid analysis to confirm purity and sequence.

NMR Experiments

For all NMR experiments, peptide concentrations were 5–10 mg/mL in a 90:10 H_2O/D_2O solution at pH 3.6. One- and two-dimensional NMR experiments were carried out using a 500 MHz Bruker AM-500 spectrometer equipped with a water suppression 5 mm ^{1}H-probe. Similar NMR experiments have recently been described in detail by our laboratory (22). NMR spectra were processed using FELIX software (version 2.30, Biosym Technologies, San Diego, CA) with a final matrix of 1K × 1K real data points. Coupling constants ($^3J_{HNC^{\alpha}_{H}}$ and $^3J_{HNC^{\beta}_{H}2}$) were measured from the double quantum filtered correlated spectroscopy (DQF-COSY) spectrum at 10°C. The temperature coefficients of the amide protons were determined from one-dimensional spectra, using plots of temperature (10–30°C) vs. chemical shift (ppm) for each of the protons.

Circular Dichroism (CD)

CD spectra were recorded with an Aviv 62DS spectropolarimeter (Lakewood, NJ) at 25°C. Peptide concentrations of 1.0 mg/mL in H_2O (0.05 cm cell path length) were used for all experiments according to methodology described previously by our laboratory (22). Each spectrum is the average of four individual scans, with averaging time of 4 sec from 190 to 280 nm in 1 nm intervals. Each spectrum was corrected for sample cell and solvent contributions and was smoothed with a third-order polynomial function.

Molecular Modeling

Molecular conformational space was searched for the Asp-containing cyclic peptide using Discover (version 2.35, Biosym Technologies, San Diego, CA) to identify conformations consistent with the experimental ROE and coupling-constant data. Calculations using consistence valence force field (Cvff) were performed on an Indigo Silicon Graphics computer (Silicon Graphics, Mountain View, CA). A detailed description of the sequence of steps used to make these calculations has been reported recently by our laboratory (22). Several conformations were selected for the final analysis using two criteria: a) interproton distance error of <0.5 Å as compared to upper and lower bound of distances from ROE data; and b) dihedral angles within 30 degrees of the calculated values from $^3J_{HNC^{\alpha}_{H}}$. Only conformers meeting these criteria were taken as viable NMR solution conformations. These conformers were then minimized with solvent molecules using the conjugate gradient method (without cross terms) until the r.m.s. derivative was ≤0.4 kcal/mole-Å. Finally, these energy-minimized structures were analyzed in terms of dihedral angles, energy and observed ROE distances. Conformers were finally clustered into one family based on structural characteristics (Φ and Ψ angles) and ROE constraints. An average structure with an interproton distance error of <0.5 Å as compared to upper and lower bound of distances from experimental ROE data and dihedral angles within 30 degrees of the calculated values from $^3J_{HNC^{\alpha}_{H}}$ was chosen.

Molecular Size Determination

The molecular radii of the peptides were calculated according to the Stokes-Einstein equation using diffusion coefficients that were experimentally determined by NMR spectroscopy (13). The relative hydrodynamic volumes of the peptides were estimated using high-resolution size exclusion chromatography performed on a Superdex Peptide 10/30 HR column (10 × 300 mm, Pharmacia Biotech, Uppsala, Sweden) as previously described by our laboratory (18). The resulting data were used to calculate a distribution coefficient (K_d) value for each peptide.

Lipophilicity Determination

The lipophilicities of the peptides were estimated by measuring their partitioning between 20 mM phosphate buffer, pH 7.4, and an immobilized artificial membrane (IAM.PC.DD column, 10 cm × 4.6 mm I.D., Regis Technologies, Inc., Morton Grove, IL) as described earlier by our laboratory (13). The resulting data were used to calculate a capacity factor (k'_{IAM}) for each peptide.

Cell Culture

Caco-2 cells were obtained from American Type Culture Collection (Rockville, MD) at passage 18. The details of the cell culture techniques used have been described earlier by our laboratory (18). In this study, the cells were used between passages 39 and 62.

Transport Studies

Caco-2 cell monolayers grown on collagen-coated polycarbonate filters (Transwells®) were used for transport experiments between days 21 and 28. The details of the transport experiments have been recently described (18). Briefly, transport experiments from the AP to BL side as well as from the BL to AP side were performed in triplicate at 37°C. Permeation of the peptides under perturbed conditions was assessed in the presence of 0.1 mM palmitoyl-DL-carnitine (PC) as described earlier (23).

HPLC Analysis

Chromatographic analyses were carried out on a Shimadzu LC-10A gradient system (Shimadzu, Inc., Tokyo, Japan). Separations were performed using a Dynamax C_{18} reversed-phase column (5 μm, 300 Å, 25 cm × 4.6 mm I.D., Rainin Instruments, Woburn, MA) equipped with a guard column. The samples were detected using a SPD-10A UV detector or a RF-535 fluorescence detector (Shimadzu, Inc., Tokyo, Japan). Fluorescence of the Trp residue was monitored at emission λ = 345 nm (excitation λ = 285 nm). Isocratic elution of the peptides was performed at a flow rate of 1 mL/min using 11–18% (v/v) acetonitrile in water with TFA (0.1%, v/v) as an ion-pairing agent.

Data Analysis

Permeability coefficients (P_{app}) of the peptides were calculated according to equation 1:

$$P_{app} = \frac{\Delta Q/\Delta t}{A \cdot c(0)} \quad (1)$$

Where $\Delta Q/\Delta t$ = linear appearance rate of mass in the receiver solution, A = cross-sectional area (i.e., 4.71 cm^2), and c(0) = initial peptide concentration in the donor compartment at t = 0.

Statistical Analysis

The results of experiments performed in triplicate are presented as mean ± S.D. Statistical significance was tested by one-way analysis of variance (ANOVA) using Tukey's family error at $p < 0.05$.

RESULTS

Physicochemical Properties

The physicochemical properties (lipophilicities, molecular radii, and hydrodynamic volumes) of the linear and cyclic hexapeptides were determined by chromatographic techniques and the results are shown in Table 1. The log k'_{IAM} values are negative for all the linear hexapeptides indicating moderate interaction between the hydrophobic regions of the immobilized phosphatidylcholine analogs and the peptides. There was a significant increase in lipophilicity observed going from the Asp-containing linear hexapeptide (log k'_{IAM} = −0.82) to the Asn containing linear hexapeptide (log k'_{IAM} = −0.37) and the Lys-containing linear hexapeptide (log k'_{IAM} = −0.11). A similar trend was observed with the cyclic hexapeptides. For example, the Asn-containing cyclic hexapeptide (log k'_{IAM} = 0.05) was more lipophilic than the Asp-containing cyclic hexapeptide (log k'_{IAM} = −0.52). The cyclic Lys-containing hexapeptide was the most lipophilic peptide in the series (log k'_{IAM} = 0.26). For each like charged pair, the cyclic hexapeptides interacted more strongly with the phospholipid stationary phase than did their linear counterparts.

The molecular radii determined by NMR experiments and the calculated distribution coefficient (K_d) determined by high-resolution size exclusion chromatography indicate that the

Table 1. Physicochemical Characteristics of Linear and Cyclic Model Hexapeptides

Compound	MW	Molecular Size		Lipophilicity	Net charge
		radius [Å][a]	K_d[b]	[log k'_{IAM}][c]	
Ac-Trp-Ala-Gly-Gly-Asp-Ala-NH_2	616	3.3	0.63	−0.82	negative
Ac-Trp-Ala-Gly-Gly-Asn-Ala-NH_2	615	3.1	0.70	−0.37	neutral
Ac-Trp-Ala-Gly-Gly-Lys-Ala-NH_2	629	3.0	0.61	−0.11	positive
Cyclo [Trp-Ala-Gly-Gly-Asp-Ala]	557	3.1	0.74	−0.52	negative
Cyclo [Trp-Ala-Gly-Gly-Asn-Ala]	556	3.0	0.94	0.05	neutral
Cyclo [Trp-Ala-Gly-Gly-Lys-Ala]	570	n.d.	0.77	0.26	positive

Note: n.d. not determined

[a] Stokes-Einstein radius calculated from the diffusion coefficient in D_2O (see Materials and Methods)

[b] K_d determined by high-resolution size exclusion chromatography

[c] Capacity factor determined from partitioning of the solute between 0.02 M phosphate buffer, pH 7.4 and an immobilized artificial membrane of phosphatidylcholine analogs (IAM.PC.DD)

cyclic peptides are similar in size when compared to their linear counterparts (Table 1).

Caco-2 Cell Transport Studies

To determine the cellular permeation characteristics of the linear and cyclic hexapeptides, their fluxes across Caco-2 monolayers were measured in the presence and absence of PC. In the absence of PC, the cyclic hexapeptides were found to be 2–3 times more able to permeate the cellular barrier from the AP to BL side as compared to their linear counterparts (Table 2). Permeation of the cyclic peptides determined in the opposite direction (i.e., BL to AP) was not significantly different from their AP to BL flux (data not shown). In the absence of PC, permeation of the positively charged linear hexapeptides through Caco-2 cell monolayers was greater than that observed for the negatively charged species, but not statistically different from the neutral species. In contrast, the ability of the cyclic peptides to permeate this cellular barrier was not influenced by the net charge of the peptide.

Earlier studies in our laboratory have shown that the average pore radius of the junctional complex can be increased by the addition of PC without completely distorting the physical barrier properties of the cell monolayer (14,23). Perturbation of the monolayer was done to compare the transport characteristics of the linear and cyclic hexapeptides under more "physiological" conditions and to elucidate the pathway by which the peptides traverse the cell monolayer (23). In the presence of 0.1 mM PC, smaller relative increases in permeation were observed for the Asp- and Asn-containing cyclic hexapeptides when compared to their linear counterparts (25-fold vs. 90-fold, respectively). For both the linear and cyclic Lys-containing hexapeptides, the flux increased approximately 20-fold under perturbed conditions.

Structural Analysis

CD Studies

In Fig. 1, the CD spectra of the linear Asp-containing hexapeptide and the cyclic Asp-containing hexapeptide are compared. The general shape and position of the extremes in the CD spectrum of the linear Asp-containing linear hexapeptide is consistent with open or random coil conformations expected for linear peptides of this size. In contrast, the cyclic Asp-containing hexapeptide displayed strong bands at 190 nm and 220 nm, which is indicative of electronic transitions of amide groups in type II β-turns (24). Similar results were obtained for the cyclic Asn- and Lys-containing peptides (data not shown).

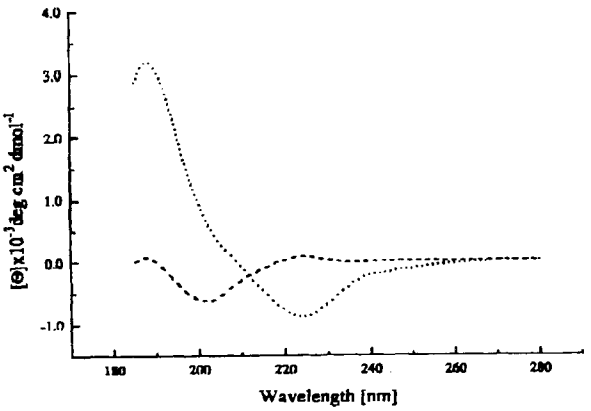

Fig. 1. CD spectra of the linear (----) and cyclic (·····) Asp-containing model hexapeptides in H_2O.

NMR Studies

In an effort to determine whether there are structural differences between the linear and cyclic hexapeptides that could help explain the differences in transport characteristics, extensive NMR studies were performed to determine the solution conformations of the linear and cyclic Asp-containing hexapeptides.

The proton chemical shifts of the cyclic Asp-containing hexapeptide were identified from the HOHAHA spectrum. Sequence-specific assignments were made from a ROESY spectrum (Fig. 2, A and B) using standard procedures (25). The one-dimensional ^1H NMR spectrum of the cyclic Asp-containing hexapeptide showed good dispersion of the chemical shifts and the coupling patterns. The amide resonance had coupling constants >5 Hz. The Gly3 and Gly4 proton resonances can be distinguished from each other by using their NH to $C^{\alpha}H$ and NH-NH sequential connectivities in the ROESY spectrum (Fig. 2, A and B). The proton resonances of Ala2 and Ala6 were distinguished by their $C^{\alpha}H$ to NH connectivities to Gly3

Table 2. Effect of Charge and Conformation on the Flux of Linear and Cyclic Model Hexapeptides in Unperturbed and Perturbed Caco-2 Monolayers

Compound	Permeability coefficients $P_{app} \times 10^8$ [cm/sec]		Relative increase in permeability[a]
	Unperturbed	Perturbed[b]	
Ac-Trp-Ala-Gly-Gly-Asp-Ala-NH_2	3.2 ± 0.3	301.9 ± 21.1	94×
Ac-Trp-Ala-Gly-Gly-Asn-Ala-NH_2	5.1 ± 0.3*	452.6 ± 47.5	89×
Ac-Trp-Ala-Gly-Gly-Lys-Ala-NH_2	4.9 ± 0.3*	107.6 ± 18.3	22×
Cyclo [Trp-Ala-Gly-Gly-Asp-Ala]	9.3 ± 0.3*	227.5 ± 23.9	24×
Cyclo [Trp-Ala-Gly-Gly-Asn-Ala]	9.5 ± 0.4*	249.5 ± 13.7	26×
Cyclo [Trp-Ala-Gly-Gly-Lys-Ala]	9.3 ± 0.1*	162.3 ± 16.8	17×

[a] When compared to the P_{app} values determined across the unperturbed cell monolayer
[b] In the presence of 0.1 mM PC
* Significant ($p < 0.05$) difference compared to the P_{app} of the linear Asp-containing hexapeptide in the unperturbed state.

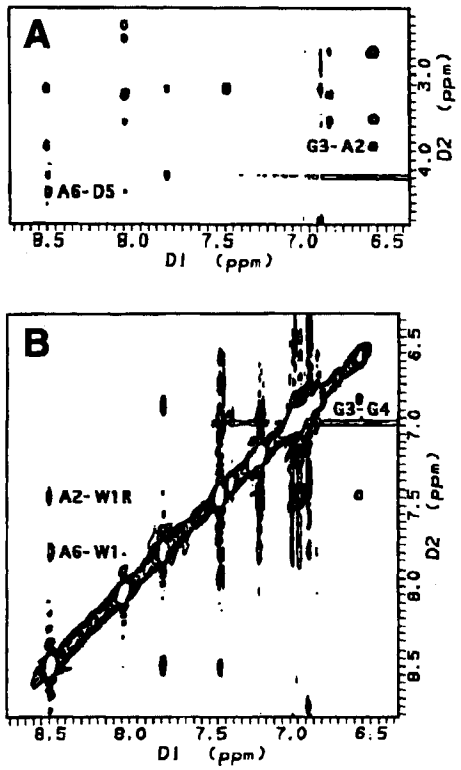

Fig. 2. Expansion of the 500 MHz ^{1}HNMR ROESY spectrum of the cyclic Asp-containing model hexapeptide in 90:10 H_2O/D_2O at 10°C. Panel A shows the amide-α region, Panel B the amide-amide region.

and Asp5, respectively. The NH of Gly4 showed through-space interactions with the NH of Gly3, while the NH of Ala6 showed through-space interactions with the NH of Trp1. The NH of Gly3 showed through-space interaction with the C$^\alpha$H of Ala2, while the NH of Ala6 showed through-space interaction with the C$^\alpha$H of Asp5. These results suggests two possible β-turns: one at Trp1-Ala2-Gly3-Gly4 and the other at Gly4-Asp5-Ala6-Trp1. The temperature coefficients of the amide proton chemical shifts are shown in Table 3. Most of the amide protons have a very large temperature coefficient of chemical shift, indicative of the presence of solvent-exposed amide protons. The NH of Trp1 showed a suppressed temperature coefficient, suggesting an intramolecularly hydrogen-bonded amide proton. The NH of Gly3 showed through-space interaction with the CH4 of the Trp aromatic ring. C$^\alpha$H enantiotopic proton resonances of Gly3 and Gly4 have a Δδ of about 0.8 and 0.3 ppm, respectively, indicating that these protons are in different chemical environments. These data also support the fact that Gly3 and Gly4 are in a region possessing secondary structure.

Similar NMR studies of the linear Asp-containing hexapeptide were also performed (data not shown). The NH of Gly4 showed through-space interactions with the NH of Gly3, while the NH of Gly3 showed through-space interactions with the C$^\alpha$H of Ala2. This result suggests a possible β-turn at Trp1-Ala2-Gly3-Gly4. However, all of the amide protons had large temperature coefficients of chemical shift, which indicates the presence of solvent-exposed amide protons. These data suggest the presence of open, random coil structures in a dynamic equilibrium with β-turn structures.

Table 3. Temperature Coefficients, Coupling Constants, and Chemical Shift Data for the Cyclic Asp-Containing Hexapeptide

Residue	Δδ/ΔT [ppb/K]	Coupling constant $^3J_{HNC\alpha H}$[Hz][a]	Chemical shift [ppm] NH	C$^\alpha$H	C$^\beta$H
Trp1	−3.0	5.88	7.79	4.15	3.14
Ala2	−12.8	7.72	8.58	3.12	1.09
Gly3	11.7	7.35	6.58	2.71/3.52	
Gly4	10.1	6.79	6.87	3.16/3.54	
Asp5	−10.3	6.62	8.05	4.36	2.40/2.56
Ala6	−11.2	6.21	8.50	4.6	1.09

[a] For glycine $^3J_{HNC\alpha H}{}^2$.

Molecular Modeling

The spectroscopic data described above strongly suggest the existence of a β-turn structure for the cyclic Asp-containing hexapeptide. From ROE-constrained molecular dynamics simulation and energy minimization studies, a family of structures was selected. These structures were consistent with the NMR data. A total of nine conformers selected from this family were superimposed onto the average structure to verify convergence with the average structure. The average r.m.s. deviation of the backbone and of all atoms was not more than 0.7 Å and 1.2 Å, respectively. The energy-minimized average structure, as shown in Fig. 3B, represents the possible major solution conformer of the cyclic Asp-containing hexapeptide. The dihedral angles Φ of all the residues are within 30 degrees of those Φ angles calculated from the coupling constant data in the average structure (Table 4) (26).

The large degree of conformational flexibility available to the linear Asp-containing hexapeptide led to a vast number of possible low energy conformers that could satisfy the NMR constraints. Based on this inherent complexity, molecular modeling of the linear Asp-containing hexapeptide was not pursued.

DISCUSSION

Earlier studies from our laboratory (13) have shown that molecular size is a major factor in determining the rate of flux of a peptide across Caco-2 cell monolayers by the paracellular route. One possible explanation for the higher permeation of the cyclic hexapeptides compared to the linear hexapeptides observed in this study might be differences in size. However, the linear and cyclic hexapeptides were shown to have almost identical size (Table 1). Therefore, the observed increase in flux of the cyclic hexapeptides could not be explained by a decrease in molecular size. Interestingly, however, the cyclic hexapeptides were more lipophilic than their linear counterparts, which might suggest a higher transcellular component to the flux of these peptides.

To determine the route by which the cyclic and linear hexapeptides traversed the Caco-2 cell monolayer, transport studies were performed in the absence and presence of PC. Previous studies carried out in our laboratory (23) have shown that a concentration of 0.1 mM PC increases the average pore radius of the junctional complex in Caco-2 cells from 4.4 ± 1.1 Å to 12.0 ± 3.2 Å, which is similar to that found in the

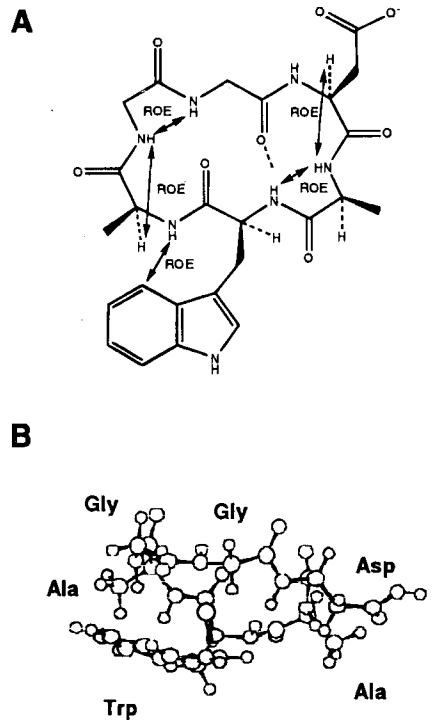

Fig. 3. Structural characterization of the cyclic Asp-containing hexapeptide. Panel A shows a schematic representation of ROE's and hydrogen bonding in the cyclic peptide as revealed by NMR spectroscopy. A major solution conformation of the cyclic Asp-containing hexapeptide was obtained by molecular dynamics simulations (Panel B). The energy-minimized average structure is consistent with an interproton distance error of <0.5 Å as compared to upper and lower bound of distances from experimental ROE data and dihedral angles within 30 degrees of the calculated values from $^3J_{HNC^{\alpha}H}$.

human jejunum (27). Permeation of the neutral and negatively charged linear hexapeptides was shown to be more sensitive (~90-fold increase) to this perturbation with PC than was that of their cyclic analogs (~20-fold increase). These results support our hypothesis that these linear hexapeptides cross the Caco-2 monolayer predominately via the paracellular route (28), whereas the cyclic analogs traverse the monolayer via the paracellular and the transcellular route (29).

In an effort to understand, at a molecular level, how structural features could explain the increased lipophilicity and higher cellular membrane permeation of the cyclic hexapeptides compared to those of the linear hexapeptides, NMR and CD studies were conducted. Spectroscopic data indicate that the Asp-containing linear hexapeptide exists in a dynamic equilibrium between random coil, open structures and β-turn structures (e.g., 4 → 1 βI-turn). In contrast, the spectroscopic data collected for the cyclic Asp-containing hexapeptide strongly suggest the existence of a two β-turn-containing structure (Fig. 3A). One turn appears to be stabilized by an intramolecular hydrogen bond between the NH of Gly4 and the C=O of Trp1. A type II β-turn structure is supported by the presence of ROE cross peaks between the NH of Gly4 and Gly3 and the NH of Gly3 to the $C^{\alpha}H$ of Ala2. The second turn appears to be stabilized by an intramolecular hydrogen bond between the NH of Trp 1 and the C=O of Gly4. The presence of this intramolecular hydrogen bonding is also supported by the low temperature coefficient of the Trp1 NH proton. The Gly3 and Gly4 NH protons exhibited a large up-field shift, which could be due to the close proximity of the Trp1 aromatic ring system. This is further supported by the observation of a ROE cross peak between the NH of Ala2 and the CH4 of the ring system (Fig. 2B). This positioning of the Trp1 side chain appears to be temperature-dependent. Formation of intramolecular hydrogen bonds, the close proximity of the Trp1 side chain to the cyclic ring structure as well as the overall amphophilic nature of the cyclic Asp-containing hexapeptide may account for an increased lipophilicity and higher cellular permeation of this peptide.

Recent studies conducted in our laboratory (18,23) have shown that two cyclic prodrugs of the hexapeptide H-Trp-Ala-Gly-Gly-Asp-Ala-OH also exhibit enhanced cellular permeation characteristics. The increased permeation across Caco-2 cell monolayers of the acyloxyalkoxycarbamate prodrug (18) can be attributed to formation of intramolecular hydrogen bonds that decrease the overall hydrogen bonding potential of the hexapeptide (22). However, for the phenylpropionic acid prodrug, the increased permeation across Caco-2 cell monolayers was attributed to incorporation of a lipophilic promoiety (23). It is important to note that the higher permeation of the cyclic peptides described in this manuscript and the cyclic prodrugs described elsewhere (18,23) can be attributed to the increased lipophilicities of the molecules. However, the structural features responsible for the changes in lipophilicity were different.

Finally, it is interesting to note that the positively charged linear hexapeptide was slightly more able to permeate Caco-2 monolayers than was the negatively charged linear hexapeptide (Table 2). This higher permeation can be explained by the presence of a negatively charged electrostatic field in the paracellular spaces (30,31), and these results are consistent with the results obtained by Adson and colleagues (15), who studied the effects of size and charge of a series of small organic-based compounds (MW ≤ 250). In contrast, the neutral, positively and negatively charged cyclic hexapeptides all had the same permeation characteristics through unperturbed Caco-2 cell monolayers (Table 2). This is a surprising observation because the affinities of the cyclic hexapeptides for the IAM.PC.DD stationary phase would have predicted the following order of permeation: positive>neutral>negative (Table 1). At this time we are unable to explain why the fluxes of the cyclic peptides do not correlate with their log k'_{IAM} values.

In summary, the spectroscopic data and molecular dynamics simulations indicate that the cyclic Asp-containing hexapep-

Table 4. Backbone Dihedral Angles (in deg) and Possible Dihedral Angles Calculated from the Coupling Constants for the Cyclic Asp-Containing Hexapeptide

Residue	Calculated Φ				Average structure Φ	Ψ
Trp1	−168	−75	24	95	−76	−100
Ala2	−160	−85	40	85	−136	−65
Gly3	−90		100		−93	40
Gly4	−130	−55	55	135	−164	−104
Asp5	−162	−78	28	85	−103	−89
Ala6	−165	−70	25	90	−85	−24

tide exhibits an amphophilic, well-defined secondary solution structure involving two β-turns. These conformational features could be responsible for the increased lipophilicity of this cyclic hexapeptide as compared to its linear counterpart. The enhanced permeation of the cyclic hexapeptides across Caco-2 monolayers, when compared to that of the linear hexapeptides, could be due to a reduction in hydrogen bonding potential and an increase in lipophilic nature, leading to an increase in flux via the transcellular route.

ACKNOWLEDGMENTS

Financial support was provided by Costar Corp., Glaxo Inc., the United States Public Health Service (GM-51633, GM-088359) and a fellowship from the Swiss National Science Foundation (G. M. P.). The authors would like to thank Dr. Seetharama D. S. Jois of the University of Kansas for his assistance with the computational chemistry.

REFERENCES

1. N. C. Wrighton, F. X. Farrell, R. Chang, A. K. Kashyap, F. P. Barbone, L. S. Mulcahy, D. L. Johnson, R. W. Barett, L. K. Jolliffe, and W. J. Dower. *Science* **273**:397–544 (1996).
2. G. M. Pauletti, S. Gangwar, G. T. Knipp, M. M. Nerurkar, F. W. Okumu, K. Tamura, T. J. Siahaan, and R. T. Borchardt. *J. Controlled Release* **41**:3–17 (1996).
3. V. H. L. Lee, R. D. Traver, and M. E. Taub. in: V. H. L. Lee (ed.), *Peptide and Protein Drug Delivery*, Marcel Dekker, New York, 1991, pp. 303–357.
4. M. J. Humphrey. in: S. S. Davis, L. Illum and E. Tomlinson (eds.), *Delivery Systems for Peptide Drugs*, Plenum Press, New York, 1986, pp. 139–151.
5. X. H. Zhou. *J. Controlled Release* **29**:239–252 (1994).
6. J. P. Yevich. in: P. Krogsgaard-Larsen and H. Bundgaard (eds.), *A Textbook of Drug Design and Development*, Harwood Academic Publishers, Langhorne, 1991, pp. 606–630.
7. R. A. Conradi, P. S. Burton, and R. T. Borchardt. in: V. Pliska, B. Testa and H. Van de Waterbeemd (eds.), *Lipophilicity in Drug Action and Toxicology*, VCH, Weinheim, 1996, pp. 233–250.
8. R. A. Conradi, A. R. Hilgers, N. F. H. Ho, and P. S. Burton. *Pharm. Res.* **9**:435–439 (1992).
9. P. S. Burton, R. A. Conradi, A. R. Hilgers, N. F. H. Ho, and L. L. Maggiora. *J. Controlled Release* **19**:87–93 (1992).
10. J. Drewe, G. Fricker, J. Vonderscher, and C. Beglinger. *Br. J. Pharmacol.* **108**:298–303 (1993).
11. S. Lundin and P. Artursson. *Int. J. Pharm.* **64**:181–186 (1990).
12. D. T. Thwaites, B. H. Hirst, and N. L. Simmons. *Pharm. Res.* **10**:674–681 (1993).
13. G. M. Pauletti, F. W. Okumu, and R. T. Borchardt. *Pharm. Res.* **14**:169–175 (1997).
14. G. T. Knipp, N. F. H. Ho, C. L. Barsuhn, and R. T. Borchardt. *Pharm. Res.* **12**:S-302 (1995).
15. A. Adson, T. J. Raub, P. S. Burton, C. L. Barsuhn, A. R. Hilgers, K. L. Audus, and N. F. H. Ho. *J. Pharm. Sci.* **83**:1529–1536 (1994).
16. D. Barlow and T. Satoh. *J. Controlled Release* **29**:283–291 (1994).
17. I. J. Hidalgo, T. J. Raub, and R. T. Borchardt. *Gastroenterology* **96**:736–749 (1989).
18. G. M. Pauletti, S. Gangwar, F. W. Okumu, T. J. Siahaan, V. J. Stella, and R. T. Borchardt. *Pharm. Res.* **13**:1615–1623 (1996).
19. H. Rink. *Tetrahedron Lett.* **28**:3787–3790 (1987).
20. G. Lu, S. Mojsov, J. P. Tam, and R. B. Merrifield. *J. Org. Chem.* **46**:3433–3436 (1981).
21. J. Diago-Meseguer and A. L. Palomo-Coll. *Synthesis* **1980**:547–551 (1980).
22. S. Gangwar, S. D. S. Jois, T. J. Siahaan, D. G. Vander Velde, V. J. Stella, and R. T. Borchardt. *Pharm. Res.* **13**:1655–1660 (1996).
23. G. M. Pauletti, S. Gangwar, B. Wang, and R. T. Borchardt. *Pharm. Res.* **14**: 11–17 (1997).
24. R. W. Woody. in: V. J. Hruby (ed.), *The Peptides*, Academic Press, New York, 1985, pp. 15–114.
25. K. Wüthrich, *NMR of Proteins and Nucleic Acids*, John Wiley & Sons, New York (1986).
26. V. F. Bystrov. *Progr. NMR Spectrosc.* **10**:41–81 (1976).
27. K. D. Fine, C. A. Santa Ana, J. L. Portes, and J. S. Fordtran. *Gastroenterology* **108**:983–989 (1995).
28. F. W. Okumu, G. M. Pauletti, D. G. Vander Velde, T. J. Siahaan, and R. T. Borchardt. *Pharm. Res.* **12**:S-302 (1995).
29. G. M. Pauletti, F. W. Okumu, D. G. Vander Velde, and R. T. Borchardt. *Pharm. Res.* **13**:S-235 (1996).
30. J. Hochman and P. Artursson. *J. Controlled Release* **29**:253–267 (1994).
31. J. R. Pappenheimer and K. Z. Reiss. *J. Memb. Biol.* **100**:123–136 (1987).